GeoHealth

RESEARCH ARTICLE
10.1029/2023GH000935

Special Section:
Geospatial data applications for environmental justice

Identification of Neighborhood Hotspots via the Cumulative Hazard Index: Results From a Community-Partnered Low-Cost Sensor Deployment

Sakshi Jain[1], Rivkah Gardner-Frolick[1], Nika Martinussen[2], Dan Jackson[3], Amanda Giang[1,2], and Naomi Zimmerman[1]

[1]Department of Mechanical Engineering, University of British Columbia, Vancouver, BC, Canada, [2]Institute for Resources Environment and Sustainability, University of British Columbia, Vancouver, BC, Canada, [3]Strathcona Residents Association, Vancouver, BC, Canada

Abstract The Strathcona neighborhood in Vancouver is particularly vulnerable to environmental injustice due to its close proximity to the Port of Vancouver, and a high proportion of Indigenous and low-income households. Furthermore, local sources of air pollutants (e.g., roadways) can contribute to small-scale variations within communities. The aim of this study was to assess hyperlocal air quality patterns (intra-neighborhood variability) and compare them to average Vancouver concentrations (inter-neighborhood variability) to identify possible disparities in air pollution exposure for the Strathcona community. Between April and August 2022, 11 low-cost sensors (LCS) were deployed within the neighborhood to measure $PM_{2.5}$, NO_2, and O_3 concentrations. The collected 15-min concentrations were down-averaged to daily concentrations and compared to greater Vancouver region concentrations to quantify the exposures faced by the community relative to the rest of the region. Concentrations were also estimated at every 25 m grid within the neighborhood to quantify the distribution of air pollution within the community. Using population information from census data, cumulative hazard indices (CHIs) were computed for every dissemination block. We found that although $PM_{2.5}$ concentrations in the neighborhood were lower than regional Vancouver averages, daily NO_2 concentrations and summer O_3 concentrations were consistently higher. Additionally, although CHIs varied daily, we found that CHIs were consistently higher in areas with high commercial activity. As such, estimating CHI for dissemination blocks was useful in identifying hotspots and potential areas of concern within the neighborhood. This information can collectively assist the community in their advocacy efforts.

Plain Language Summary Historically marginalized communities can experience environmental injustice due to disproportionately high air pollution relative to other communities. The Strathcona neighborhood in Vancouver is of particular concern due to its proximity to the Port of Vancouver, major roads and railways, and a high proportion of Indigenous and low-income households. Here, we assess hyperlocal air quality patterns in Strathcona and compare them to average Vancouver concentrations to assess potential air quality inequity. Between April and August 2022, 11 low-cost sensors (LCS) measuring $PM_{2.5}$, O_3, and NO_2 were deployed in community backyards. The daily average concentrations were compared to those in other Vancouver neighborhoods. Concentrations were also estimated at every 25m grid within the neighborhood using ordinary kriging, a relatively simple spatial interpolation technique. Using Census population data, cumulative hazard indices (CHIs, which combine $PM_{2.5}$, O_3, and NO_2 in a single metric) were computed for every dissemination block. We found that daily NO_2 concentrations and summer O_3 concentrations consistently higher than in other Vancouver neighborhoods. Although CHIs varied daily, CHIs were consistently higher in areas with high commercial activity. The kriging model was more easily implemented than traditional land use regression models, and may be useful to communities struggling to interpret LCS network data.

Key Points:

- Mapping the cumulative hazard index (CHI) is a useful way for communities to summarize complex outputs from low-cost air quality sensors
- The NO_2 concentrations in the study area were consistently higher than other Metro Vancouver neighborhoods
- The western and eastern peripheries (high commercial density) of the study domain were the dominant hotspots, depending on wind direction

Supporting Information:

Supporting Information may be found in the online version of this article.

Correspondence to:

N. Zimmerman,
nzimmerman@mech.ubc.ca

Citation:

Jain, S., Gardner-Frolick, R., Martinussen, N., Jackson, D., Giang, A., & Zimmerman, N. (2024). Identification of neighborhood hotspots via the cumulative hazard index: Results from a community-partnered low-cost sensor deployment. *GeoHealth*, *8*, e2023GH000935. https://doi.org/10.1029/2023GH000935

Received 25 AUG 2023
Accepted 19 DEC 2023

Author Contributions:

Conceptualization: Sakshi Jain, Rivkah Gardner-Frolick
Data curation: Sakshi Jain, Rivkah Gardner-Frolick
Formal analysis: Sakshi Jain
Funding acquisition: Sakshi Jain, Rivkah Gardner-Frolick, Naomi Zimmerman

1. Introduction

It is well established that air pollution exposure has many associated health impacts, which can range from asthma to premature mortality (Brauer et al., 2016; Brook et al., 2010; Di et al., 2017; Pope III, 2002). Even low levels of air pollution can be detrimental to human health; according to a recent Health Effects Institute report, there is no concentration below which the negative health impacts of $PM_{2.5}$ (particles with diameter of 2.5 μm or smaller) are not observed (Brauer et al., 2022).

Investigation: Sakshi Jain, Rivkah Gardner-Frolick, Nika Martinussen
Methodology: Sakshi Jain, Amanda Giang, Naomi Zimmerman
Project administration: Dan Jackson, Amanda Giang, Naomi Zimmerman
Resources: Dan Jackson
Supervision: Amanda Giang, Naomi Zimmerman
Visualization: Sakshi Jain
Writing – original draft: Sakshi Jain
Writing – review & editing: Amanda Giang, Naomi Zimmerman

The cumulative effect of chronic exposure to multiple pollutants can exacerbate these health impacts, even at levels below national benchmarks (Xia & Tong, 2006). Additionally, cumulative effects of different pollutants can highlight different areas of concern than when assessments are conducted for individual pollutants separately (Giang & Castellani, 2020; Su et al., 2009). Since people breathe a mixture of air pollutants, cumulative assessment can be more representative of human exposure. In Canada, the AQHI (Air Quality Health Index) is used for health assessment of air quality, which includes cumulative effects of $PM_{2.5}$, nitrogen dioxide (NO_2) and ozone (O_3) (Gutenberg, 2014).

Air pollution concentrations have small-scale variations (Beelen et al., 2013; M. Wang et al., 2013) and can vary greatly in space and time (Baldwin et al., 2015; Eeftens et al., 2012; Li et al., 2016; M. Wang et al., 2013). Socially or economically marginalized communities, including low-income, people of color and Indigenous communities, are often disproportionately exposed to air pollution (Clark et al., 2014; Morello-Frosch & Jesdale, 2006; Pinault et al., 2016; Wiebe, 2016). In addition to environmental exposure, marginalized groups often also experience social and political marginalization, which can be due to inequitable access to healthcare and input on policy decisions, further increasing their vulnerability to the health impacts of air pollution (O'Neill et al., 2003). As such, risks arising from air pollution exposure are not equitably distributed.

Canada, and British Columbia in particular, generally have good air quality, but there are areas that are disproportionately impacted by higher concentrations and that have a greater number of potentially vulnerable populations (Giang et al., 2022; Jerrett et al., 2001; Kershaw et al., 2013; Pinault et al., 2016). One such area in British Columbia is the Downtown Eastside and Strathcona neighborhood in Vancouver, from both a geographic and demographic perspective. Geographically, in addition to typical Vancouver sources of air pollution like residential wood burning and construction, Strathcona and the Downtown Eastside are located next to the Port of Vancouver. The Port of Vancouver is the largest port in Canada and in the top five in North America by tonnes of cargo (Conway, 2012), and as such has significant associated ship, truck, and rail traffic. These port activities are associated with emissions of particulate matter ($PM_{2.5}$, particles with diameter $\leq$2.5 μm) and nitrogen oxides (NO_x: NO and NO_2) (Gobbi et al., 2020). The neighborhood is also adjacent to major roadways and Downtown Vancouver, which further exacerbates air pollution via light-duty vehicle emissions of NO_x. From a demographic perspective, Strathcona and the Downtown Eastside have a high proportion of low-income, unhoused, immigrant, and Indigenous people (City of Vancouver, 2020a). The diversity and potential social vulnerability of many residents in these neighborhoods, combined with the likely higher than regional air pollution resulting from various local sources, means that the people of Strathcona and Downtown Eastside may be disproportionately exposed to air pollution.

However, assessing the cumulative hazard of air pollution in Strathcona is not feasible with the current regulatory monitoring network. The City of Vancouver has only one air quality monitoring station that measures all pollutants, making it difficult to identify areas of concern within the city or specific neighborhoods. The sparse distribution of regulatory monitors is typically due to the high capital and maintenance costs involved (Castell et al., 2017; Maag et al., 2018; Si et al., 2020). One potential solution for obtaining more spatially representative data is the use of low-cost air quality sensors (LCS). LCS cost a fraction of regulatory stations (Castell et al., 2017) and can operate on battery or solar power. This provides an opportunity for a denser sensor network, capable of capturing small-scale variations in pollutant levels (Bi et al., 2020; Minet et al., 2017; Piedrahita et al., 2014; Snyder et al., 2013).

In this study, we partnered with the Strathcona Residents Association (SRA) and deployed 11 multi-pollutant low-cost sensors in the Strathcona and Downtown Eastside neighborhoods in Vancouver for a duration of 6 months in 2022, with the aim of capturing small-scale spatial variability in pollutant concentrations. By comparing the measured concentrations with the average concentrations in the broader Vancouver region, we investigated the effectiveness of using LCS to identify disparities in air quality. Additionally, we calculated cumulative hazard indices (CHIs) as a method to identify hotspots and areas of concern within the neighborhood based on the principles of cumulative hazard assessment.

2. Methodology

2.1. Study Area

Strathcona is a neighborhood located within the City of Vancouver and is classified as one of the 22 planning areas (City of Vancouver, 2020b), with a population of approximately 12,600, as of the 2016 census (City of

Figure 1. The Strathcona and Downtown Eastside neighborhoods of Vancouver that were studied in this work (black dashed line; 3 km × 1 km). Green lines are the rail lines within the study area, and orange lines highlight the major roads (line sources of air pollution). Red markers identify major point sources of air pollution (port, industries). Blue star markers are the deployment locations of the air quality sensors (RAMPs).

Vancouver, 2020a). The neighborhood encompasses mixed land use types, including residential, commercial, and industrial areas. Residential areas consist of privately owned homes, as well as collective dwellings that house 20% of the population, including senior residences and single room occupancy (SRO) hotels (City of Vancouver, 2020a). Strathcona is surrounded by industrial facilities on its south and east sides (produce terminal, recycling facility, small chemical processing plants), and a shipping yard on its north side (Centerm and Vanterm container terminals of Port of Vancouver) (Strathcona Residents Association, 2021). The neighborhood's western border adjoins Downtown Vancouver, another planning area of the City of Vancouver. The portion of Downtown Vancouver adjacent to Strathcona is called the Downtown Eastside (DTES), which is home to Chinatown and Gastown, the historic center of Vancouver (City of Vancouver, 2020b). Figure 1 shows the locations of major roadways, rail lines and industrial sources within the study area (dashed black line).

In Strathcona, approximately 10% of the residents identify as Indigenous, which is the highest proportion of any neighborhood in Vancouver (city average = 2.4%) (City of Vancouver, 2020a). More than half (52%) of the population in Strathcona have a household income below the national poverty line, which is notably higher than the citywide average of 20% (City of Vancouver, 2020a). Furthermore, according to a report by the City of Vancouver, about 22% of the residents in Strathcona are unhoused or living in SROs, and are not represented in these census demographics (City of Vancouver, 2020a). Strathcona and the DTES area together account for 52% of the total unhoused individuals in the City of Vancouver (Mauboules, 2020).

2.2. Community Partner: Strathcona Residents Association

The Strathcona Residents Association (SRA) is a volunteer-based nonprofit organization that represents residents and workers in the Strathcona neighborhood of Vancouver. In 2019, the Port of Vancouver initiated construction activities to expand the Centerm and Vanterm container terminals, aiming to boost their cargo handling capacity by 50% (GCT Global Container Terminals Inc, 2019). This expansion is projected to lead to an increase in the volume of ships, trains, and trucks passing by or through Strathcona. In 2021, the SRA conducted a survey among its residents to assess their perspectives on air quality in the neighborhood. The survey revealed that out of 181 participants, 84% viewed the air quality as gradually declining. Furthermore, 79% of the participants expressed being very concerned about exhaust emissions from heavy-duty diesel trucks transporting shipping containers through the neighborhood (Strathcona Residents Association, 2021). Survey participants were also asked about their level of concern about the health effects arising from exposure to transportation

Table 1
Mean and Standard Deviation (SD) of the Performance Metrics After Applying the Calibration Models to the Withheld Testing Data From the Collocation Period*

	R^2		MAE		CvMAE	
Pollutant	Mean	SD	Mean	SD	Mean	SD
$PM_{2.5}$	0.65	0.17	1.82 μg m^{-3}	0.80 μg m^{-3}	0.30	0.06
NO_2	0.61	0.08	3.92 ppb	0.44 ppb	0.22	0.02
O_3	0.84	0.06	3.03 ppb	0.53 ppb	0.25	0.04

Note. *SD= $\sqrt{\frac{\sum(x_i-\bar{x})^2}{n-1}}$ where $n = 11$ RAMPs, x_i is the performance metric for an individual RAMP, and $\bar{x}$ is the average performance metric across all 11 RAMPs. Detailed RAMP-by-RAMP performance metrics are provided in Supporting Information S1.

and vehicle-related air pollution in the area. Headache, nose and throat irritation, asthma, and lung cancer were ranked as "very concerning" by approximately 40% of participants. In explaining their concerns, participants described a range of observed and perceived health effects related to nose and throat irritation, asthma, and chronic sinus infection. While there was no direct measurement data of traffic-related air pollution (TRAP) in Strathcona at the time of the survey, a 2015–2017 study at the Clark Drive Near-Road Monitoring Station approximately 2 km from Strathcona highlighted that this station had higher concentrations of TRAP, including NO_2, nitric oxide (NO), black carbon (BC), $PM_{2.5}$, and ultrafine particles (UFP), compared to other monitoring sites in the region. NO_2 specifically was approximately 40% higher at the Clark Drive Station, with clear correlations to diesel traffic volumes. Furthermore, higher concentrations were more frequent at the Clark Drive station and there were more exceedances of Metro Vancouver's air quality objectives than at other regional monitoring sites (Metro Vancouver, 2020).

Recognizing these concerns, the study team at the University of British Columbia (UBC) partnered with the SRA to assess the community's concerns about their air quality. We proposed a comprehensive plan to collect air quality data, sought approval from the UBC Research Ethics Board (UBC Ethics ID: H21-02425) and secured funding through the UBC Public Scholar Initiative. The Public Scholars Initiative supports doctoral students whose research supports and contributes to public good.

2.3. Low-Cost Sensors

The low-cost pollutant monitoring system used for this work was the Remote Air Quality Monitoring Platform (RAMP, SENSIT Technologies), which cost approximately CAD 4000 (less than 5% of the cost for a full suite of regulatory grade monitors measuring the same pollutants; typical regulatory monitors cost >CAD 20,000 per pollutant). The RAMP package combines a power supply (battery-operated, solar powered or both), a SIM card slot for online transmission of data via cellular network, a memory card for data storage, and gas and particle sensors in a weatherproof enclosure. The RAMP includes a commercial nephelometer to measure $PM_{2.5}$ (Plantower PMS5003), and electrochemical sensors for NO_2 and O_3 (Alphasense NO2-B43F and Alphasense Ox-B431). It also records temperature (T) and relative humidity (RH). The RAMP records data with a 15-s sampling resolution.

Since LCS systems need routine calibration across the full range of expected meteorological conditions and pollutant concentrations during deployment to achieve good performance (Cross et al., 2017; Masson et al., 2015; Mead et al., 2013; Moltchanov et al., 2015; Pang et al., 2017), we collocated the RAMP sensors at Metro Vancouver's Clark Drive Near-Road regulatory monitoring station before and after the campaign for a total of 62 days (collocation dates pre-campaign: 24 February–31 March 2022; post-campaign: 22 January–5 February 2023). Calibration models were built for each RAMP using previously published calibration techniques (Malings et al., 2019, 2020) (a multiple linear regression model for $PM_{2.5}$ and hybrid random-forest-multiple-linear regression model for NO_2 and O_3) on 75% of the combined pre- and post-collocation data set (remainder set aside for model testing) after down-averaging the data to 15-min resolution to reduce the effect of noise (Malings et al., 2020). Separating the data into training and testing data sets was done by removing every 4th day from the collocation data set for testing. The performance of the calibration models was assessed on the testing data set using two metrics: R^2 (coefficient of determination, linear least squares regression of predicted vs. observed concentrations; higher is better) and MAE (mean absolute error; lower is better). We also reported relative error in the calibration models by calculating CvMAE (coefficient of variation of MAE; lower is better) using Equation 1. The calibration models had varied performance across different pollutants, reported in Table 1. Detailed performance metrics for individual RAMP units are provided in Table S1 of the Supporting Information S1.

$$CvMAE = \frac{\frac{1}{n}\sum_{i=1}^{n}|Calibrated\ value_i - Observed\ value_i|}{Average\ observed\ concentrations} \quad (1)$$

2.4. Site Selection

The design of this study was rooted in our belief that community members are the most knowledgeable of their spaces. As such, we conducted a walking tour of the neighborhood with representatives from the SRA to choose sampling locations. During this tour, we identified potential emission sources (major roadways, rail lines, construction), and receptor locations (cycling routes, parks, schools, senior housing facilities, Indigenous daycares, and unhoused communities). Informed by the insights gained from the walking tour, the SRA compiled a list of potential hosts for the study and contacted them. There were two key logistical requirements for inclusion in the study, which were communicated to the residents and business owners. First, the chosen residences or businesses needed to have an outdoor area with access to a power supply to ensure continuous operation of the RAMPs. Second, residents were required to occupy their homes for at least 75% of the time, or businesses needed to be operational for at least 75% of working days, in order to grant us access to the RAMPs for maintenance purposes.

Eleven prospective residential households in the neighborhood expressed interest in participating. In alignment with COVID-19 protocols, we conducted virtual tours with each host to obtain their consent and discuss the logistics associated with deploying air quality sensors at their respective households. After careful consideration, a total of seven hosts were selected for RAMP deployment based on their proximity to pollution sources or their representation of vulnerable populations. The selected deployment locations were as follows: (a) near a rail line to monitor rail emissions, (b) on Hastings Road, a major roadway in the neighborhood, to monitor truck and road traffic-related pollutants, (c) across from Strathcona Park to represent individuals engaging in outdoor physical activities, (d) Union Street, a prominent biking route, (e) two RAMPs near an elementary school and a community center and (f) near a cluster of low-income households. All RAMPs were deployed at ground level, approximately 3 m above the ground to represent ground level exposure.

In addition to the residential deployments, four RAMPs were deployed at businesses in the study area, to provide additional insights into the neighborhood air quality, particularly in areas influenced by commercial activities and community-focused establishments. These businesses themselves did not generate significant levels of indoor air pollution (e.g., from cooking or wood burning) that could significantly influence outdoor concentrations. The RAMP placements at commercial businesses were as follows: (a) second floor of a yoga studio in Chinatown, located on Main Street, which experiences high commercial foot and vehicle traffic, (b) a community garden on Hastings Street, (c) the rooftop located on the fourth floor of a community-center hub on Main Street, and (d) the rooftop located on the fourth floor of a veteran's housing society. Ideally, it would have been preferable to deploy all of the RAMPs at ground level (i.e., approximately 3 m above ground). However, due to safety concerns related to theft prevention and logistics of sensor installation, these organizations did not have access to suitable locations on ground level. As a result, two RAMPs were deployed at an elevated area, approximately 10–15 m high. Figure 1 shows the approximate location of the study RAMPs (blue stars).

2.5. Data Collection and Processing

RAMPs were deployed in the backyards of residents and businesses in Strathcona and Downtown Eastside between April and November of 2022 to collect $PM_{2.5}$, NO_2, and O_3 concentrations. Regulatory data for comparison was obtained for four Metro Vancouver neighborhood monitoring stations in Burnaby (stations Burnaby South and Burnaby Kensington), North Vancouver (station: Mahon Park) and Richmond (station: Richmond South). Population data for each dissemination block (DB; smallest geographic area for which population counts are disseminated in Canada) was extracted from Canadian census data, visualized in Figure S1 of the Supporting Information S1.

Metro Vancouver's (MV) ambient air quality objective (Metro Vancouver, 2023) for each pollutant was used as the denominator for comparison, with $PM_{2.5}$, NO_2, and O_3 benchmark values of 25 μg m^{-3}, 60 ppb (daily maximum 1-hr concentration) and 62 ppb (daily maximum 8-hr concentration), respectively (Table 2). To facilitate analysis, we down-averaged the calibrated data to match the time resolutions and criteria of the benchmark concentrations. For example, 15-min calibrated NO_2 concentrations were down-averaged to 1-hr concentrations, and then the daily maximum 1-hr concentrations were used as the estimated value for each calendar day.

Since there are measurement uncertainties associated with the RAMP sensors (Table 1), the comparison between the average regional MV concentrations was conducted with a data set that incorporated these sensor uncertainties. To accomplish this, we estimated absolute percent residuals for each decile concentration bin and

Table 2
$PM_{2.5}$ (Daily Average), NO_2 (Daily 1-hr Maximum) and O_3 (Daily 8-hr Maximum) MV Air Quality Objectives and Reported Concentrations Across Four MV Stations

Station	$PM_{2.5}$ (μg m^{-3})	NO_2 (ppb)	O_3 (ppb)
Air Quality Objectives	25[a]	60[b]	62[c]
Burnaby South	5.1 (2.3–8.9)	16.1 (9.7–23.2)	28.4 (20.1–37.5)
Burnaby Kensington	4.6 (1.9–7.7)	16.0 (9.2–24.8)	26.4 (18.9–34.7)
Richmond South	4.4 (1.8–7.6)	16.3 (9.2–23.7)	29.4 (21.1–39.3)
Mahon Park	4.3 (1.9–7.3)	16.7 (7.8–28.3)	25.7 (17.5–35.3)
Average (MV Stations)	4.6 (2.0–6.5)	16.3 (9.0–25.0)	27.5 (19.4–36.7)
Average (RAMPs)	4.6 (2.2–6.4)	21.7 (14.9–28.7)	28.1 (17.4–39.2)

Note. The values reported are averages during the deployment period, and the numbers in brackets are 10th and 90th percentiles. [a]Achievement based on rolling average. [b]Achievement based on annual 98th percentile of the daily maximum 1-hr concentration, averaged over three consecutive years. [c]Achievement based on annual 4th highest daily maximum 8-hr concentration, averaged over three consecutive years.

subtracted them or added them to the corresponding calibrated concentrations to create upper and lower bounds, respectively. This approach was employed because the error in RAMP measurements depend on the ambient concentration, with greater uncertainties observed at lower concentrations (Malings et al., 2019; Zimmerman et al., 2018). The error-informed data set was generated through the following steps:

1. The RAMP collocation data during the calibration (after correction with the calibration models) was divided into decile bins and absolute percent residuals were calculated for each bin (Equation 2).

$$\%\ error_{bin} = \frac{|Calibrated\ concentration - Reference\ concentration|}{Reference\ concentration} * 100\% \quad (2)$$

2. The median absolute % error corresponding to the decile bin of the calibrated concentration was subtracted (lower bound) or added (upper bound) for the deployment period to generate the error-informed data sets (Equations 3 and 4). Box plots of the relative % error are shown in Figure S2 of Supporting Information S1.

$$Lower\ bound = Calibrated\ concentration\ (1 - error_{bin}\ (\%)) \quad (3)$$

$$Upper\ bound = Calibrated\ concentration\ (1 + error_{bin}\ (\%)) \quad (4)$$

To assess the full extent of sensitivity to LCS measurement uncertainty, we also calculated lower and upper bounds by using the 5th and 95th percentiles of the of the error fraction distributions from Figure S2 (Supporting Information S1) in the corresponding bin. These results are provided in Supporting Information S1 (Figure S3).

2.6. Spatial Modeling

Air pollution studies have routinely used various interpolation techniques to estimate concentrations in unsampled areas (Gressent et al., 2020; Munir et al., 2021). Interpolation involves applying mathematical processes to the measured concentrations to estimate values across a continuous spatial field. One commonly used interpolation technique is kriging (Buzzelli et al., 2003; Nguyen & Marshall, 2018; Xu et al., 2019), which takes into account auto-correlation in the data, unlike other techniques such as inverse distance weighting or spline.

Kriging operates on the principle that nearby points have a higher influence on an estimate than distant points (Munir et al., 2021). It also takes clustering into account, whereby clusters of points are given less weight to reduce bias in predictions. The kriging process involves two steps: (a) fitting a variogram, which is a visual representation of the covariance between each pair of points in the sampled data, to determine the spatial covariance; and (b) using the spatial covariance to derive weights for interpolating values (Equation 5).

$$z_y = \sum_{i=1}^{N} \lambda_i z_x \tag{5}$$

In Equation 5, N is the number of measured values, z_y is the predicted value z at point y, λ is the kriging weights and z_x is the observed concentration z at sampled point x.

However, kriging suffers from assumptions of both linearity (uniformity in all directions) and stationarity (stationary mean and variance across the study space) (Olea, 1999), and is less accurate than other more complex methods that incorporate additional data, such as land use regression models (Adam-Poupart et al., 2014; Mercer et al., 2011). Nevertheless, ordinary kriging has been widely used in environmental justice research due to its ease of implementation and lack of additional data requirements (Buzzelli et al., 2003; Gardner-Frolick et al., 2022; Jerrett et al., 2001; Nguyen & Marshall, 2018; Xu et al., 2019). For this project, we opted for ordinary kriging as a simpler spatial method to prioritize solutions that communities could potentially independently construct and that do not rely on complex data inputs. In this work, kriging models were applied to estimate daily concentrations of $PM_{2.5}$, NO_2, and O_3 at each 25 m grid distance and were then averaged to concentrations at each dissemination block.

2.7. Estimating Cumulative Air Pollution Impacts

Composite measures of sustainability have previously been calculated by aggregating indicators (Kang et al., 2002; Munda, 2005) using approaches such as multiplicative, additive, binary/threshold and mixed aggregation (Zhou et al., 2006). These approaches have also been adopted to measure the unequal distribution of environmental hazards caused by multiple pollutants (Giang & Castellani, 2020; Su et al., 2009). For this work, we aggregated multiple air pollutants to calculate a cumulative hazard index (CHI); the CHI is then used to identify hotspots within the study area. CHI was calculated using both the multiplicative and additive methods (Equations 6 and 7).

$$CHI_{Multiplicative,j} = \prod_{i=1}^{3} r_{i,j}^{\text{norm}} \tag{6}$$

$$CHI_{Additive,j} = \sum_{i=1}^{3} r_{i,j}^{\text{norm}} \tag{7}$$

In Equations 6 and 7, $r_{i,j}^{\text{norm}}$ is the normalized hazard index (HI) of the pollutant i at dissemination block j. $r_{i,j}^{\text{norm}}$ is calculated by first dividing the air pollutant concentration by the Metro Vancouver air quality objective (benchmark value) to account for different measurement units (Munda, 2005), and then scaling the data by the population so that all the pollutants are on the same scale (Su et al., 2009). The process is shown in Equation 8, where $c_{i,j}$ is the pollutant i concentration at the dissemination block j, s_i is the benchmark value for the pollutant, p is the population of dissemination block j and $r_{i,j}$ is the normalized pollutant i concentration.

$$r_{i,j}^{\text{norm}} = \frac{r_{i,j}}{r_{pw-avg}} \quad where \quad r_{i,j} = \frac{c_{i,j}}{s_i} \quad and \quad r_{pw-avg} = \frac{\sum_j r_{i,j} \times p_j}{\sum_j p_j} \tag{8}$$

The multiplicative CHI was built with the assumption that there is an interaction between different pollutants (Villa & McLeod, 2002). We also calculated the Additive CHI (Equation 7), as it assumes no interaction between pollutants (Shrestha et al., 2016) and therefore can also indicate areas where individual pollutants are high.

The $r_{(i,j)}^{\text{norm}}$ values were scaled to have a mean of 1, therefore, the mean Multiplicative CHI is expected to be 1 ($1 \times 1 \times 1$ for the three pollutants) and the mean Additive CHI is expected to be 3 ($1 + 1 + 1$ for the three pollutants). Higher Multiplicative CHI values indicate a higher cumulative impact of pollutants in a particular area, whereas higher Additive CHI values indicate areas where individual pollutants exhibit high concentrations and contribute to a higher cumulative impact. This approach allows for the assessment of hyper-local air quality patterns (intra-neighborhood variability) and can be used to identify hotspots. We have chosen not to population-weight the CHIs themselves, however, this could be an additional step that one might take to assess cumulative

impacts. Given how the data have been processed, the interpretation of absolute CHI is less important than relative changes in CHI. There is no benchmark CHI level, it is simply a tool to help communities identify potential hotspots that can be used as part of ongoing advocacy with local regulatory agencies or as evidence to strategically inform more advanced monitoring.

Additionally, while we have chosen a similar form of the CHI to previous publications (Giang & Castellani, 2020; Su et al., 2009), the choice of CHI weighting schemes should ideally be developed through a combination of expert input and stakeholder deliberation (Su et al., 2009). For example, the Canadian Air Quality Health Index (AQHI) is weighted based on epidemiological evidence for excess mortality risk from Canadian cities, and not for morbidity which may be more of a concern (Giang & Castellani, 2020; Stieb et al., 2008).

3. Results and Discussion

3.1. Data Summary

During the campaign, six of the eleven total RAMPs experienced some degree of malfunction, due to a combination of power loss, sensor degradation, or failures in the data logging/transmission system. Unfortunately, we were unable to address the malfunctioning sensors effectively, due to various reasons, including scheduling conflicts with hosts. Two RAMPs underwent sensor degradation and reported data with quality issues (e.g., uncharacteristically high, zero, or no readings) and were removed. Furthermore, at the beginning of a renovation period at the community garden, the charging cable for one of the RAMP sensors was cut. We decided against redeploying the RAMP at this location to avoid the influence of construction on the overall data collection. Consequently, only 53% of the originally planned data was collected. This data underwent QA/QC via visual inspection to ensure there was no influence of short-lived highly localized pollution events from smoking or barbecuing; due to the careful siting decisions away from cooking areas and smoking areas we did not observe any irregular pollution concentrations from residents' activities.

Since missing data wasn't sporadic (e.g., sensors malfunctioned and were never fixed), we applied criteria for data completeness for inclusion in the analysis. Specifically, we considered only those days with at least eight functioning RAMP sensors, which corresponds to a data completeness of 75% (a benchmark suggested in the low-cost sensor guidelines provided by the US Environmental Protection Agency (US EPA, Williams et al., 2014)). As a result, our final data set meeting the completeness criteria consisted of 119 days of RAMP data, collected between 27 April 2022 and 23 August 2022. All days between those dates had at least 8 RAMP monitors online.

During the period when all 11 RAMPs were operational, we conducted Monte Carlo simulations to assess the sensitivity of the model to the presence or absence of each sensor. We predicted daily concentrations at every grid by removing one sensor at a time and compared these predictions to the predictions when all RAMPs were used. We reported the p-value of the mean differences in the two data sets (difference in predicted concentrations when test RAMP is excluded and when test RAMP is included), and repeated this process 11 times for 11 RAMPs. Through these simulations, we identified three RAMPs as critical, as their absence resulted in statistically significant differences ($p < 0.05$) in the predictions. While two of the critical sensors remained operational throughout the campaign period, one sensor stopped working on June 10th. It is likely that having all critical sensors operational would have led to more accurate predictions, which could potentially affect the CHI estimates. We acknowledge this as a limitation of our work and emphasize the importance of identifying critical sensors early on to ensure data completeness in future studies. Furthermore, it is worth noting that two sensors were deployed at an elevated height, which may have impacted the measured pollutant concentrations. A study by Wu et al. (2002) reported $PM_{2.5}$ concentration decays of up to 73% at a height of 19 m. As such, concentrations at the ground level are likely to be higher than those reported at 10–15 m. The effect of height and associated microclimate was not considered in our analysis, and we recognize this as a limitation of our work.

All sensors across all days recorded data below the Metro Vancouver Air Quality Objectives (Table 2). The average 24-hr $PM_{2.5}$ concentration was 4.6 μg m^{-3} [10th–90th percentile: 2.2–6.4 μg m^{-3}], with highest concentrations observed on June 30th when a fire broke out in the neighborhood (Kerr, 2022). The average daily 1-hr maximum NO_2 across all sensors was 21.7 ppb [10th–90th percentile: 14.9–28.7 ppb], with diurnal peaks observed around 7–8 a.m. only on weekdays (see Figure S4 of Supporting Information S1 for diurnal plots), suggesting a contribution from morning rush hour traffic. The average daily 8-hr maximum O_3 concentration was 28.1 ppb [10th–90th percentile: 17.4–39.2 ppb], with diurnal peaks observed in the afternoon. This is expected, as

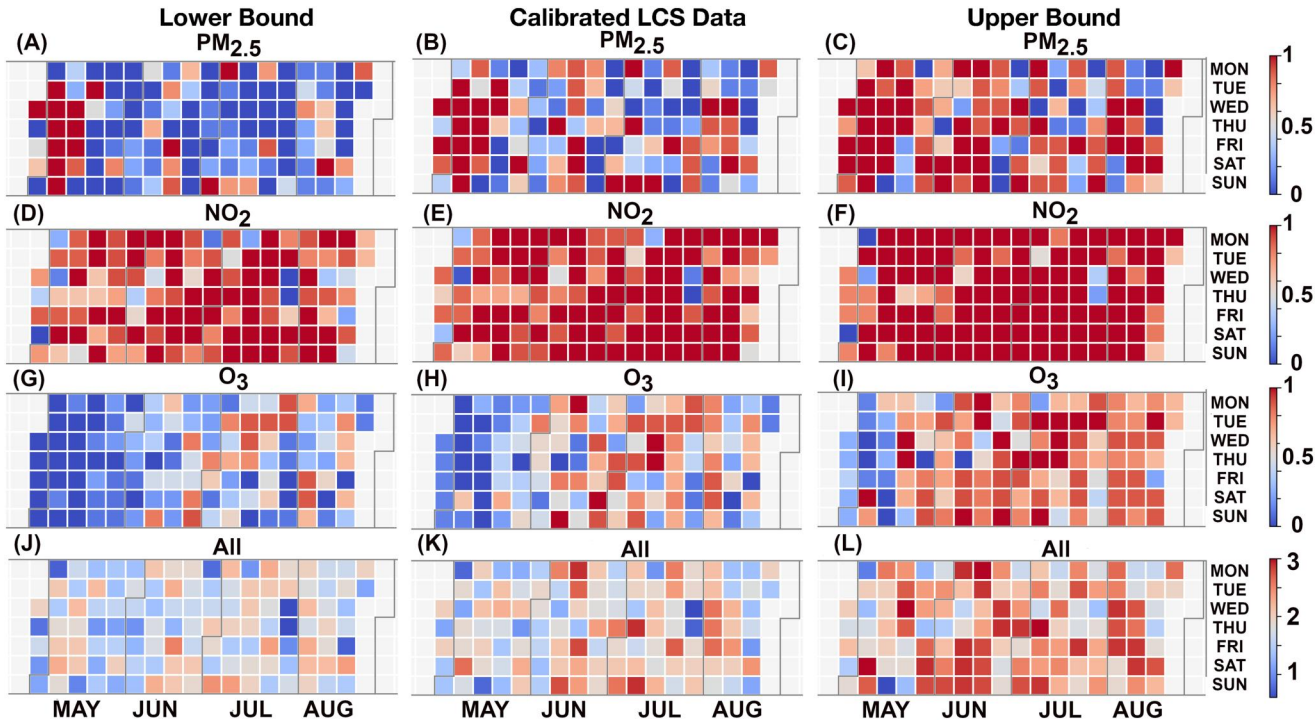

Figure 2. Calendar plots for the ratio of sensors exceeding average MV regional concentrations for lower bound, calibrated LCS and upper bound data sets for $PM_{2.5}$ (plots A-C), NO_2 (plots D–F) and O_3 (plots G–I). Ratio = 0 (blue) indicates that none of the RAMPs exceeded MV concentrations, whereas ratio = 1 (red) indicates that all the operational RAMPs exceeded MV averages. The calendar plot in the bottom row (plots J–L) shows the ratio of sensors exceeding average MV regional concentrations for the three pollutants together (additive form; combined results from the three plots above). Ratio = 0 (blue) indicates that no pollutant across all the RAMPs exceeded MV concentrations, whereas ratio = 3 (red) indicates that all the pollutants across all the RAMPs exceeded MV concentrations.

tropospheric ozone is a secondary air pollutant that is formed photochemically in the atmosphere from the reactions of NO_x and volatile organic compounds (VOCs) (Seinfeld & Pandis, 2016). By comparison, across four neighborhood Metro Vancouver regulatory monitoring stations in the region, average $PM_{2.5}$, NO_2, and O_3 concentrations were 4.6 μg m^{-3}, 16.3 ppb, and 27.5 ppb, respectively (Table 2).

3.2. Inter-Neighborhood Variability

We conducted a comparison between the concentrations of each pollutant across all operational RAMPs within the neighborhood and the average concentrations measured at four neighborhood regulatory monitoring stations in the MV region (Table 2). The comparison was made on the same time-scale as the air quality objectives. Specifically, we compared $PM_{2.5}$ concentrations on a daily basis, NO_2 concentrations on the maximum 1-hr concentration over the day, and O_3 concentrations on the maximum 8-hr concentration over the day. To account for the measurement uncertainties associated with the RAMP sensors, we also compared the error-informed data sets (Section 2.5). We then calculated the number of RAMPs (and the corresponding fraction of RAMPs) that exceeded the average MV regional concentrations for each pollutant individually, as well as for all pollutants combined.

Figure 2 panels a–c, d–f, and g–i illustrate the fraction of RAMPs exceeding the average regional concentration in Metro Vancouver for $PM_{2.5}$, NO_2, and O_3, respectively. A pollutant was considered as "exceeding" the regional average in our study domain if more than 50% of the RAMPs exceeded the average concentrations in the MV region (ratio ≥0.5 in panels a–i). During the 119-day study period, the concentrations of O_3 and $PM_{2.5}$ in the neighborhood exceeded the average concentrations in the MV region on 58 (lower—upper bound: 28–92) and 62 (lower—upper bound: 36–87) days, respectively. On the other hand, NO_2 concentrations in the neighborhood exceeded the average concentrations on almost every day (113 days; lower—upper bound: 105–117), with daily 1-hr maximum NO_2 concentrations being on average over 5 ppb higher in Strathcona (Table 2). Using the lower bound error-informed RAMP NO_2 concentrations still resulted in an average excess 3 ppb exposure. This

Table 3
Multiplicative and Additive CHIs for RAMPs and Metro Vancouver Stations

ID	Total days (n)	Multiplicative CHI	Additive CHI
RAMP 1001	100	1.71 (0.99–2.63)	3.68 (3.07–4.32)
RAMP 1002	119	2.08 (1.25–3.40)	3.83 (3.26–4.56)
RAMP 1004	119	1.38 (0.80–2.08)	3.33 (2.81–3.89)
RAMP 1005	96	3.38 (0.87–4.80)	4.31 (2.87–5.11)
RAMP 1008	119	1.45 (0.88–2.39)	3.37 (2.88–4.07)
RAMP 1009	119	1.51 (0.89–2.31)	3.47 (3.01–4.02)
RAMP 1011	108	1.20 (0.72–1.95)	3.18 (2.71–3.83)
RAMP 1012	96	1.26 (0.59–2.06)	3.44 (2.84–4.15)
RAMP 1039	44	1.32 (1.01–1.75)	3.31 (3.05–3.63)
RAMP 1040	28	1.01 (0.77–1.19)	3.02 (2.76–3.21)
Average (RAMPs)		1.63 (0.85–2.50)	3.49 (2.91–4.11)
Burnaby South	119	1.36 (0.68–2.11)	3.34 (2.71–4.05)
Richmond South	119	1.17 (0.63–1.78)	3.18 (2.72–3.66)
Mahon Park	119	1.11 (0.44–2.22)	3.04 (2.38–3.95)
Average (MV Stations)		1.22 (0.57–2.08)	3.19 (2.59–3.91)

Note. The values report the average during the deployment period, and the numbers in brackets are 10th and 90th percentiles. Approximate locations of each RAMP ID are available on Zenodo (Jain et al., 2023).

indicates that residents in the study area experienced higher NO_2 concentrations compared to the regional average. The higher NO_2 concentrations are likely also the primary contributing factor in the higher O_3 concentrations observed in the summer months; the majority of the days where ≥50% of the RAMP O_3 measurements exceeded the MV regional averages were on summer days when the sunlight needed for photochemical conversion of NO_x to O_3 was most intense. For a detailed breakdown of the number of days each RAMP exceeded the MV averages, please refer to Table S2 in Supporting Information S1. Additionally, at least two pollutants simultaneously exceeded the average MV concentrations on 93 out of the total 119 days, reinforcing the hypothesis that neighborhood residents disproportionately experience poorer air quality.

The persistently high levels of NO_2 in the area, even after accounting for sensor uncertainties, raise concerns about air quality. Vehicle traffic in the Lower Fraser Valley is the primary source of NO_x, contributing approximately 63% to the overall pollution levels (Doerksen et al., 2020). Among vehicular sources, heavy-duty diesel trucks are considered the most significant contributor to TRAP. This is supported by a study conducted by Metro Vancouver at the Clark Drive Near-Road monitoring station (approximately 3 km from the nearest deployed RAMP, and where the RAMPs were calibrated), that found that the vehicle type, particularly heavy-duty diesel trucks, rather than total traffic volume, was the main predictor of the amount and type of air contaminants associated with major roadways in the area (Doerksen et al., 2020). In 2017 at the Clark Drive station, which can be used as a proxy for our study area, heavy-duty diesel trucks comprised 18% of the total vehicle fleet, six times higher than the regional fleet percentage of 3% (Doerksen et al., 2020). The planned expansions at Vanterm and Centerm, set to increase the port capacity by 50% (GCT Global Container Terminals Inc, 2019), are expected to result in a further rise in shipping-related traffic, including trucks, within the study area. It is important to consider the potential consequences of these increases on TRAP, as the elevated TRAP not only suggests the potential for increased NO_2 concentrations but also has implications on elevated O_3 levels, especially during the summer months (reflected in Figure 2h; June–August).

We also assessed inter-neighborhood variability in cumulative pollution by calculating Multiplicative and Additive CHIs for calibrated data from 10 of the RAMPs deployed in Strathcona and three MV stations (Table 3). One RAMP and one MV station (Burnaby Kensington) were excluded from the analysis due to no residents in the dissemination block where the monitor was sited (population = 0). Among the three MV stations, the Burnaby

South station had higher CHIs, likely due to its proximity to a major roadway (Kingsway street). Among the 10 RAMPs in Strathcona, only two had lower average CHIs (either Multiplicative and Additive) than the average across the MV stations (RAMP 1011 and RAMP 1040). It is worth highlighting that one of these two RAMPs (RAMP 1040) recorded data for less than 25% of the study duration, and likely poorly represents the entire study period. To better compare RAMP 1040 and the MV stations, we isolated the period when RAMP 1040 was online, and separately calculated the average CHI across MV stations. We found that for these 28 days, the MV CHIs were comparable to RAMP 1040 (average Multiplicative MV CHI = 1.01 [0.59, 1.56]). As such, this reinforces the overall finding, that the Strathcona and Downtown Eastside neighborhood generally experiences elevated pollution levels when compared to other neighborhoods in the Metro Vancouver region, and the cleanest locations (RAMP 1040 and RAMP 1011) matched the MV station averages (i.e., there was nowhere sampled with cleaner air than the MV station averages).

The results of these analyses support the community's concerns regarding poorer air quality and highlight the potential of LCS monitoring as a useful tool for identifying disparities in air quality. These findings can also support communities in their advocacy efforts for improved air quality by providing quantitative evidence of their concerns. Targeted policies aimed at reducing emissions from traffic sources, particularly trucks, could help mitigate overall air pollution levels in the neighborhood due to disproptionate impact of high NO_2 concentrations on our findings. One specific policy approach for which members of the SRA have been advocating is the phasing out of pre-2007 trucks, as part of the Vancouver Fraser Port Authority's Rolling Truck Age Program. This initiative aims to address the higher emissions from older trucks, which generally do not have modern NO_x emission control technologies installed (Khalek et al., 2015).

Previous studies have consistently shown that Downtown Vancouver and surrounding neighborhoods have higher annual average NO_2 concentrations compared to the broader MV area (Giang & Castellani, 2020; Pinault et al., 2016; Setton et al., 2008). R. Wang et al. (2013) reported an average concentration of 10.8 ppb in 2010, estimated using land use regression for each dissemination area; the highest concentrations were in Downtown Vancouver. Giang and Castellani (2020) used annual air quality data sets for 2012 and estimated concentrations for each dissemination area in the City of Vancouver. They reported average concentrations in the study area for NO_2 and O_3 to be approximately 27 and 30 ppb, higher than city averages by 70% and 40%, respectively (city averages: NO_2 = 15.9 ppb; O_3 = 21.4 ppb). A study conducted by MV of 2017 air quality reported approximately 9 and 6 ppb higher concentrations of NO_2 at the Clark Drive and Downtown monitoring stations, respectively, when compared to compared to five other neighborhood MV stations (average = 13 ppb) (Doerksen et al., 2020). Our study, conducted in 2022, shows a promising reduction in average NO_2 and O_3 concentrations in the MV region compared to R. Wang et al. (2013), Giang and Castellani (2020), and Doerksen et al. (2020) (average NO_2 = 9.2 ppb and O_3 = 18.8 ppb), however, the Strathcona and DTES areas still experience higher NO_2 concentrations (average = 14.2 ppb across 11 RAMPs). Additionally, the reported averages of our work are for summer only. Since NO_2 concentrations are typically higher in winter due to lower atmospheric mixing height and increased heating (Doerksen et al., 2020; Roberts–Semple et al., 2012), the average annual concentrations are likely to be higher. Furthermore, Doerksen et al. (2020) reported an increase in annual NO_2 concentrations from 2015 to 2017 across 7 out of 8 monitoring station in the region (Doerksen et al., 2020).

3.3. Intra-Neighborhood Variability

We calculated Multiplicative and Additive CHIs for each dissemination block and each day of the study period to assess the intra-neighborhood variability within the neighborhood (Figure 3). Note that if a dissemination block had no residents (population = 0) it is rendered as a blank space in Figure 3. Spatial maps generated using both additive and multiplicative CHIs exhibited similar patterns, although the additive CHIs showed generally less spatial variation (coefficient of variations: Additive CHI = 0.05; Multiplicative CHI = 0.16; more descriptive statistics in Table S3 of the Supporting Information S1), which aligns with the findings from previous studies (Giang & Castellani, 2020; Shrestha et al., 2016; Su et al., 2009). The reasoning for the spatial homogeneity of the additive CHI is that the additive CHI is more influenced by a single high pollutant than the multiplicative CHI. Essentially, the minimum additive CHI will tend toward the NO_2 HI as a lower limit when other pollutant HIs are low; in the case of multiplicative CHI, if other pollutant HIs are low, this will scale the NO_2 hazard index as well, since they are multiplied together. As such, we expect to see a wider range of CHIs in the multiplicative CHI calculations.

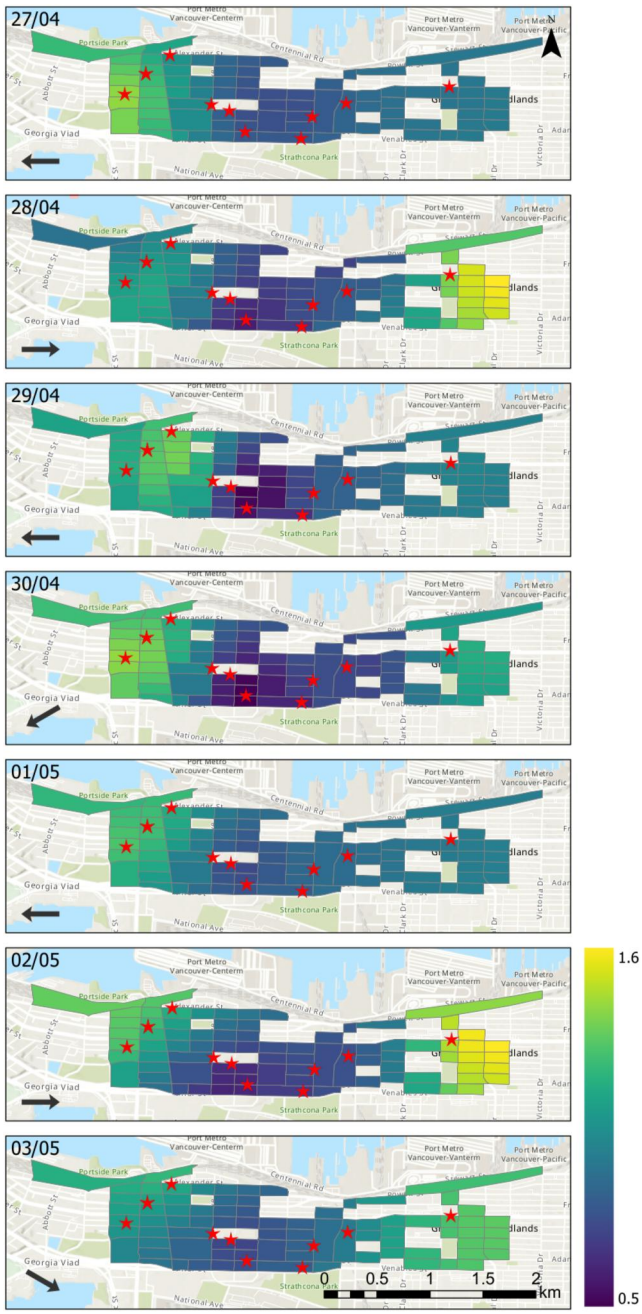

Figure 3. Multiplicative CHI for the first week of deployment (27 April–3 May 2022). The black arrow in the bottom left corner of each subplot is the prevailing wind direction for the day. The LCS locations are overlaid as red stars.

Based on the CHI analysis, two areas were consistently identified as hotspots during the study period: the western and eastern periphery of the study area. The western periphery of the study region includes Main Street and Chinatown, and has a high residential and commercial density (population distribution in each DB is shown in Figure S1 of the Supporting Information S1), and a large population of unhoused individuals (Mauboules, 2020). The eastern periphery of the study area includes Commercial Drive, which has high foot traffic and road traffic due to high commercial density. The prevailing wind in the region blows from the east (land breeze), followed by winds from the west (sea breeze; see Figure S5 of the Supporting Information S1). This influence of wind is highlighted in Figure 3, which illustrates the Multiplicative CHI over a 1-week period. Depending on the day and time of day, different parts of the neighborhood are located in the downwind direction of dense commercial zones and experienced elevated CHI values. Aggregated CHIs over the whole deployment period for both Multiplicative and Additive CHIs are shown in Figures S6 and S7 of the Supporting Information S1. We also assessed these patterns using a 25 m grid in addition to dissemination blocks, since the dissemination blocks are not uniform in size (Figure S8 in Supporting Information S1); we observed similar patterns using both the 25 m grid and dissemination blocks, with hotspots in the western and eastern periphery depending on prevailing wind direction. To identify potential local source hotspots, we also generated CHI maps on days with the lowest recorded daily average wind speed (8 km hr^{-1}) when local transport of emissions would be lowest (Figure S9 in Supporting Information S1). The low wind speed mapping showed more local hotspots on the western periphery and near the industrial sources and rail lines illustrated in Figure 1.

The results of this analysis provide valuable insights into the occurrence of air pollution hotspots within the neighborhood. This could support community advocacy with regulatory agencies or provide preliminary evidence for more sophisticated monitoring campaigns. Residents could also use these findings to make informed decisions and minimize their exposure to pollutants. For instance, they may choose to exercise in parks located in less polluted areas in the middle of the neighborhood rather than those at the periphery, or choose bike routes that avoid elevated pollution areas within the neighborhood. Building on this work, one potential application is the development of a community dashboard that incorporates simple geospatial models like kriging, for communities to use should they choose to deploy a network of sensors. This dashboard would allow residents to input their own pollution and location data and visualize the hotspots and CHIs in their specific areas. Such a tool would empower individuals to take proactive measures to protect their health and make informed choices regarding their daily activities, and help with the pervasive issue of interpreting the complex multi-pollutant data reported by low-cost sensors. One caveat to this analysis is that there is substantial uncertainty in the identified eastern periphery hotspot due to only one sensor being deployed in that area. As such, this particular hotspot may be biased from nearby local traffic emissions. For communities planning to conduct a similar analysis, one potential recommendation could be to build these geospatial kriging maps via iteration; zones that are initially identified as potential hotspots after a few weeks of deployment could be confirmed through strategic sensor re-deployment across the hotspot.

A few studies have investigated the intra-neighborhood variability of individual pollutants. Shakya et al. (2019) assessed five separate neighborhoods in Philadelphia (USA) for $PM_{2.5}$ using mobile sampling conducted for 2–4 hr each day. In a day, the study found variability within a neighborhood to be as high as 17 μg m^{-3}. Tunno

et al. (2012) assessed intra-neighborhood $PM_{2.5}$ variability in Braddock (Pittsburgh, USA) using mobile monitoring and found that average measured concentrations varied between 42 and 55 μg m^{-3} within the neighborhood. In line with these findings, our study collected data from 11 different locations within the neighborhood and found daily average $PM_{2.5}$ concentrations to vary by as much as 7 μg m^{-3}. Li et al. (2019) conducted mobile sampling in Pittsburgh (USA) and reported that NO_2 exhibited within-neighborhood spatial variation, with hotspots elevated by up to 20 ppb above the regional background concentrations (7 ppb). This supports the findings of our study; we observed intra-neighborhood variability as high as 36 ppb in daily maximum 1-hr NO_2 concentration over the deployment period. However, although intra-neighborhood variability has previously been studied for individual pollutants, we could not identify any studies that addressed hotspots for cumulative effects of different pollutants. Furthermore, previous studies have often relied on mobile monitoring to assess intra-neighborhood variability, which may not be easily adopted by communities due to the associated costs and technical expertise required to establish and maintain such mobile monitors.

4. Conclusion

This work reported the intra- and inter-neighborhood variability in air pollution within the Strathcona and DTES neighborhood in Vancouver. To achieve this, we deployed and collected pollution data using 11 LCS placed within the neighborhood to capture various sources and receptors. The findings of this study support the hypothesis that LCS can serve as valuable tools for air pollution monitoring and neighborhood-level assessments for communities, and highlighted that some neighborhoods in a city may experience disproportionately higher pollutant concentrations.

The findings of this study provide evidence supporting the use of LCS by communities to gain a better understanding of their local air quality. We conducted a comparison of pollutant concentrations within the neighborhood with the average regional levels, which provided valuable insights into the extent to which the neighborhood concentrations deviated. Moreover, these findings support the community's concerns regarding air quality and can potentially serve as a basis for advocating for improved traffic-related policies. The study also highlights the significance of LCS as a valuable tool that communities can use to identify areas of concern within their neighborhoods and make informed decisions toward improving their overall exposure to pollutants. The Centerm expansion was completed in Spring 2023 and the Vanterm expansion is ongoing. To confirm the suspected influence of port-related truck traffic on local air quality in Strathcona, we recommend that this analysis be repeated to monitor trends over time. In January 2023, the Port of Vancouver launched the Strathcona Area Air Quality Study, which includes 18 LCS monitoring locations deployed for 2 years (Vancouver Fraser Port Authority, 2023). The method proposed here can be applied to this data set to meet this recommendation.

There are several limitations to this work. First, as previously mentioned, two sensors were deployed at an elevated height. As such, the study did not consider the impact of height and micro-climate in identifying hotspots. Additionally, this study focuses on investigating intra-neighborhood variability by using daily values, aligning with the time-resolution of the air quality objectives set by Metro Vancouver. However, exploring sub-daily concentrations could provide insights into different areas of concern. Lastly, we used kriging to create spatial models and identify hotspots as a reduced-complexity solution that may be adoptable by communities. While kriging is a useful tool for estimating concentrations in unsampled areas, it is inherently less accurate than more complex models. As such, for future work where accuracy is important, employing more sophisticated models, such as land use models, may be preferable.

Conflict of Interest

The authors declare no conflicts of interest relevant to this study.

Data Availability Statement

The calibrated low-cost sensor data needed to build the kriging maps and calculate cumulative hazard indices, as well as metadata on sensor locations, and the dissemination block populations pertinent to our study area are available on Zenodo (Jain et al., 2023).

Acknowledgments
This work was supported by the Public Scholars Initiative (PSI) at the University of British Columbia. Funding for this work was provided, in part, from the Canada Research Chairs program [CRC-2018-0257]. The authors are grateful to the volunteers in the Strathcona and Downtown Eastside neighborhoods of Vancouver for hosting the sensors and to members of the community for their meaningful conversations and support.

References

Adam-Poupart, A., Brand, A., Fournier, M., Jerrett, M., & Smargiassi, A. (2014). Spatiotemporal modeling of ozone levels in Quebec (Canada): A comparison of kriging, land-use regression (LUR), and combined Bayesian maximum entropy–LUR approaches. *Environmental Health Perspectives*, *122*(9), 970–976. https://doi.org/10.1289/ehp.1306566

Baldwin, N., Gilani, O., Raja, S., Batterman, S., Ganguly, R., Hopke, P., et al. (2015). Factors affecting pollutant concentrations in the near-road environment. *Atmospheric Environment*, *115*, 223–235. https://doi.org/10.1016/j.atmosenv.2015.05.024

Beelen, R., Hoek, G., Vienneau, D., Eeftens, M., Dimakopoulou, K., Pedeli, X., et al. (2013). Development of NO_2 and NO_x land use regression models for estimating air pollution exposure in 36 study areas in Europe—The ESCAPE project. *Atmospheric Environment*, *72*, 10–23. https://doi.org/10.1016/j.atmosenv.2013.02.037

Bi, J., Stowell, J., Seto, E. Y., English, P. B., Al-Hamdan, M. Z., Kinney, P. L., et al. (2020). Contribution of low-cost sensor measurements to the prediction of $PM_{2.5}$ levels: A case study in Imperial County, California, USA. *Environmental Research*, *180*, 108810. https://doi.org/10.1016/j.envres.2019.108810

Brauer, M., Brook, J. R., Christidis, T., Chu, Y., Crouse, D. L., Erickson, A., et al. (2022). *Mortality–air pollution associations in low exposure environments (MAPLE): Phase 2. Research report*. Health Effects Institute.

Brauer, M., Freedman, G., Frostad, J., van Donkelaar, A., Martin, R. V., Dentener, F., et al. (2016). Ambient air pollution exposure estimation for the global burden of disease 2013. *Environmental Science & Technology*, *50*(1), 79–88. https://doi.org/10.1021/acs.est.5b03709

Brook, R. D., Rajagopalan, S., Pope, C. A., Brook, J. R., Bhatnagar, A., Diez-Roux, A. V., et al. (2010). Particulate matter air pollution and cardiovascular disease: An update to the scientific statement from the American heart association. *Circulation*, *121*(21), 2331–2378. https://doi.org/10.1161/CIR.0b013e3181dbece1

Buzzelli, M., Jerrett, M., Burnett, R., & Finklestein, N. (2003). Spatiotemporal perspectives on air pollution and environmental justice in Hamilton, Canada, 1985–1996. *Annals of the Association of American Geographers*, *93*(3), 557–573. https://doi.org/10.1111/1467-8306.9303003

Castell, N., Dauge, F. R., Schneider, P., Vogt, M., Lerner, U., Fishbain, B., et al. (2017). Can commercial low-cost sensor platforms contribute to air quality monitoring and exposure estimates? *Environment International*, *99*, 293–302. https://doi.org/10.1016/j.envint.2016.12.007

City of Vancouver. (2020a). Strathcona: Neighbourhood social indicators profile 2020. (Technical Report). Retrieved from vancouver.ca/files/cov/social-indicators-profile-strathcona.pdf

City of Vancouver. (2020b). Vancouver: City social indicator profile 2020. (Technical Report). Retrieved from https://vancouver.ca/files/cov/social-indicators-profile-city-of-vancouver.pdf

Clark, L. P., Millet, D. B., & Marshall, J. D. (2014). National patterns in environmental injustice and inequality: Outdoor NO_2 air pollution in the United States. *PLoS One*, *9*(4), e94431. https://doi.org/10.1371/journal.pone.0094431

Conway, K. C. (2012). North American port analysis: Beyond Post-Panamax Basics to logistics. The counselors of real estate. Retrieved from https://cre.org/real-estate-issues/north-american-port-analysis-beyond-post-panamax-basics-logistics/

Cross, E. S., Williams, L. R., Lewis, D. K., Magoon, G. R., Onasch, T. B., Kaminsky, M. L., et al. (2017). Use of electrochemical sensors for measurement of air pollution: Correcting interference response and validating measurements. *Atmospheric Measurement Techniques*, *10*(9), 3575–3588. https://doi.org/10.5194/amt-10-3575-2017

Di, Q., Wang, Y., Zanobetti, A., Wang, Y., Koutrakis, P., Choirat, C., et al. (2017). Air pollution and mortality in the medicare population. *New England Journal of Medicine*, *376*(26), 2513–2522. https://doi.org/10.1056/NEJMoa1702747

Doerksen, G., Howe, K., Thai, A., & Reid, K. (2020). Metro Vancouver near-road air quality monitoring study.

Eeftens, M., Beelen, R., de Hoogh, K., Bellander, T., Cesaroni, G., Cirach, M., et al. (2012). Development of land use regression models for $PM_{2.5}$, $PM_{2.5}$ absorbance, PM_{10} and PM_{coarse} in 20 European study areas; results of the ESCAPE project. *Environmental Science & Technology*, *46*(20), 11195–11205. https://doi.org/10.1021/es301948k

Gardner-Frolick, R., Boyd, D., & Giang, A. (2022). Selecting data analytic and modeling methods to support air pollution and environmental justice investigations: A critical review and guidance framework. *Environmental Science & Technology*, *56*(5), 2843–2860. https://doi.org/10.1021/acs.est.1c01739

GCT Global Container Terminals Inc. (2019). Analysis of capacity options on the west coast of Canada. (Technical Report No. BQ-0894). Retrieved from https://iaac-aeic.gc.ca/050/documents/p80054/130087E.pdf

Giang, A., Boyd, D. R., Ono, A. J., & McIlroy-Young, B. (2022). Exposure, access, and inequities: Central themes, emerging trends, and key gaps in Canadian environmental justice literature from 2006 to 2017. *Canadian Geographer*, *66*(3), 434–449. https://doi.org/10.1111/cag.12754

Giang, A., & Castellani, K. (2020). Cumulative air pollution indicators highlight unique patterns of injustice in urban Canada. *Environmental Research Letters*, *15*(12), 124063. https://doi.org/10.1088/1748-9326/abcac5

Gobbi, G. P., Di Liberto, L., & Barnaba, F. (2020). Impact of port emissions on EU-regulated and non-regulated air quality indicators: The case of Civitavecchia (Italy). *Science of the Total Environment*, *719*, 134984. https://doi.org/10.1016/j.scitotenv.2019.134984

Gressent, A., Malherbe, L., Colette, A., Rollin, H., & Scimia, R. (2020). Data fusion for air quality mapping using low-cost sensor observations: Feasibility and added-value. *Environment International*, *143*, 105965. https://doi.org/10.1016/j.envint.2020.105965

Gutenberg, S. (2014). Demystifying the air quality health index. *Canadian Pharmacists Journal/Revue des Pharmaciens du Canada*, *147*(6), 332–334. https://doi.org/10.1177/1715163514552560

Jain, S., Gardner-Frolick, R., Martinussen, N., Jackson, D., Giang, A., & Zimmerman, N. (2023). Supplementary data for "Identification of neighborhood hotspots via the cumulative hazard index: Results from a community-partnered low-cost sensor deployment" [Dataset]. Zenodo, *1.0*. https://doi.org/10.5281/zenodo.8284426

Jerrett, M., Burnett, R. T., Kanaroglou, P., Eyles, J., Finkelstein, N., Giovis, C., & Brook, J. R. (2001). A GIS–environmental justice analysis of particulate air pollution in Hamilton, Canada. *Environment and Planning A: Economy and Space*, *33*(6), 955–973. https://doi.org/10.1068/a33137

Kang, S. M., Kim, M. S., & Lee, M. (2002). The trends of composite environmental indices in Korea. *Journal of Environmental Management*, *64*(2), 199–206. https://doi.org/10.1006/jema.2001.0529

Kerr, T. (2022). *Fire destroys value village in east Vancouver*. Global News. Retrieved from https://globalnews.ca/news/8958070/fire-value-village-east-vancouver/

Kershaw, S., Gower, S., Rinner, C., & Campbell, M. (2013). Identifying inequitable exposure to toxic air pollution in racialized and low-income neighbourhoods to support pollution prevention. *Geospatial Health*, *7*(2), 265. https://doi.org/10.4081/gh.2013.85

Khalek, I. A., Blanks, M. G., Merritt, P. M., & Zielinska, B. (2015). Regulated and unregulated emissions from modern 2010 emissions-compliant heavy-duty on-highway diesel engines. *Journal of the Air & Waste Management Association*, *65*(8), 987–1001. https://doi.org/10.1080/10962247.2015.1051606

Li, H. Z., Dallmann, T. R., Gu, P., & Presto, A. A. (2016). Application of mobile sampling to investigate spatial variation in fine particle composition. *Atmospheric Environment*, *142*, 71–82. https://doi.org/10.1016/j.atmosenv.2016.07.042

Li, H. Z., Gu, P., Ye, Q., Zimmerman, N., Robinson, E. S., Subramanian, R., et al. (2019). Spatially dense air pollutant sampling: Implications of spatial variability on the representativeness of stationary air pollutant monitors. *Atmospheric Environment: X*, *2*, 100012. https://doi.org/10.1016/j.aeaoa.2019.100012

Maag, B., Zhou, Z., & Thiele, L. (2018). A survey on sensor calibration in air pollution monitoring deployments. *IEEE Internet of Things Journal*, *5*(6), 4857–4870. https://doi.org/10.1109/JIOT.2018.2853660

Malings, C., Tanzer, R., Hauryliuk, A., Kumar, S. P. N., Zimmerman, N., Kara, L. B., et al. (2019). Development of a general calibration model and long-term performance evaluation of low-cost sensors for air pollutant gas monitoring. *Atmospheric Measurement Techniques*, *12*(2), 903–920. https://doi.org/10.5194/amt-12-903-2019

Malings, C., Tanzer, R., Hauryliuk, A., Saha, P. K., Robinson, A. L., Presto, A. A., & Subramanian, R. (2020). Fine particle mass monitoring with low-cost sensors: Corrections and long-term performance evaluation. *Aerosol Science and Technology*, *54*(2), 160–174. https://doi.org/10.1080/02786826.2019.1623863

Masson, N., Piedrahita, R., & Hannigan, M. (2015). Quantification method for electrolytic sensors in long-term monitoring of ambient air quality. *Sensors*, *15*(10), 27283–27302. https://doi.org/10.3390/s151027283

Mauboules, C. (2020). Homelessness & supportive housing strategy. Retrieved from https://council.vancouver.ca/20201007/documents/pspc1presentation.pdf

Mead, M., Popoola, O., Stewart, G., Landshoff, P., Calleja, M., Hayes, M., et al. (2013). The use of electrochemical sensors for monitoring urban air quality in low-cost, high-density networks. *Atmospheric Environment*, *70*, 186–203. https://doi.org/10.1016/j.atmosenv.2012.11.060

Mercer, L. D., Szpiro, A. A., Sheppard, L., Lindström, J., Adar, S. D., Allen, R. W., et al. (2011). Comparing universal kriging and land-use regression for predicting concentrations of gaseous oxides of nitrogen (NO_x) for the Multi-Ethnic Study of Atherosclerosis and Air Pollution (MESA Air). *Atmospheric Environment*, *45*(26), 4412–4420. https://doi.org/10.1016/j.atmosenv.2011.05.043

Metro Vancouver. (2020). Metro Vancouver near-road air quality monitoring study. (Technical Report). Retrieved from https://metrovancouver.org/services/air-quality-climate-action/Documents/near-road-air-quality-monitoring-study-technical-report-2015-2017.pdf

Metro Vancouver. (2023). Air aware and small sensors. Retrieved from http://www.metrovancouver.org/services/air-quality/action/air-aware/Pages/default.aspx

Minet, L., Gehr, R., & Hatzopoulou, M. (2017). Capturing the sensitivity of land-use regression models to short-term mobile monitoring campaigns using air pollution micro-sensors. *Environmental Pollution*, *230*, 280–290. https://doi.org/10.1016/j.envpol.2017.06.071

Moltchanov, S., Levy, I., Etzion, Y., Lerner, U., Broday, D. M., & Fishbain, B. (2015). On the feasibility of measuring urban air pollution by wireless distributed sensor networks. *Science of the Total Environment*, *502*, 537–547. https://doi.org/10.1016/j.scitotenv.2014.09.059

Morello-Frosch, R., & Jesdale, B. M. (2006). Separate and unequal: Residential segregation and estimated cancer risks associated with ambient air toxics in U.S. Metropolitan areas. *Environmental Health Perspectives*, *114*(3), 386–393. https://doi.org/10.1289/ehp.8500

Munda, G. (2005). "Measuring sustainability": A multi-criterion framework. *Environment, Development and Sustainability*, *7*(1), 117–134. https://doi.org/10.1007/s10668-003-4713-0

Munir, S., Mayfield, M., & Coca, D. (2021). Understanding spatial variability of NO_2 in urban areas using spatial modelling and data fusion approaches. *Atmosphere*, *12*(2), 179. https://doi.org/10.3390/atmos12020179

Nguyen, N. P., & Marshall, J. D. (2018). Impact, efficiency, inequality, and injustice of urban air pollution: Variability by emission location. *Environmental Research Letters*, *13*(2), 024002. https://doi.org/10.1088/1748-9326/aa9cb5

Olea, R. A. (1999). Ordinary kriging. In *Geostatistics for engineers and Earth scientists* (pp. 39–65). Springer US. https://doi.org/10.1007/978-1-4615-5001-3_4

O'Neill, M. S., Jerrett, M., Kawachi, I., Levy, J. I., Cohen, A. J., Gouveia, N., et al. (2003). Health, wealth, and air pollution: Advancing theory and methods. *Environmental Health Perspectives*, *111*(16), 1861–1870. https://doi.org/10.1289/ehp.6334

Pang, X., Shaw, M. D., Lewis, A. C., Carpenter, L. J., & Batchellier, T. (2017). Electrochemical ozone sensors: A miniaturised alternative for ozone measurements in laboratory experiments and air-quality monitoring. *Sensors and Actuators B: Chemical*, *240*, 829–837. https://doi.org/10.1016/j.snb.2016.09.020

Piedrahita, R., Xiang, Y., Masson, N., Ortega, J., Collier, A., Jiang, Y., et al. (2014). The next generation of low-cost personal air quality sensors for quantitative exposure monitoring. *Atmospheric Measurement Techniques*, *7*(10), 3325–3336. https://doi.org/10.5194/amt-7-3325-2014

Pinault, L., Crouse, D., Jerrett, M., Brauer, M., & Tjepkema, M. (2016). Spatial associations between socioeconomic groups and NO_2 air pollution exposure within three large Canadian cities. *Environmental Research*, *147*, 373–382. https://doi.org/10.1016/j.envres.2016.02.033

Pope, C. A., III. (2002). Lung cancer, cardiopulmonary mortality, and long-term exposure to fine particulate air pollution. *Journal of the American Medical Association*, *287*(9), 1132. https://doi.org/10.1001/jama.287.9.1132

Roberts–Semple, D., Song, F., & Gao, Y. (2012). Seasonal characteristics of ambient nitrogen oxides and ground–level ozone in metropolitan northeastern New Jersey. *Atmospheric Pollution Research*, *3*(2), 247–257. https://doi.org/10.5094/APR.2012.027

Seinfeld, J. H., & Pandis, S. N. (2016). *Atmospheric chemistry and physics: From air pollution to climate change* (3rd ed.). Wiley-Interscience.

Setton, E. M., Keller, C. P., Cloutier-Fisher, D., & Hystad, P. W. (2008). Spatial variations in estimated chronic exposure to traffic-related air pollution in working populations: A simulation. *International Journal of Health Geographics*, *7*(1), 39. https://doi.org/10.1186/1476-072X-7-39

Shakya, K. M., Kremer, P., Henderson, K., McMahon, M., Peltier, R. E., Bromberg, S., & Stewart, J. (2019). Mobile monitoring of air and noise pollution in Philadelphia neighborhoods during summer 2017. *Environmental Pollution*, *255*, 113195. https://doi.org/10.1016/j.envpol.2019.113195

Shrestha, R., Flacke, J., Martinez, J., & Van Maarseveen, M. (2016). Environmental health related socio-spatial inequalities: Identifying "hotspots" of environmental burdens and social vulnerability. *International Journal of Environmental Research and Public Health*, *13*(7), 691. https://doi.org/10.3390/ijerph13070691

Si, M., Xiong, Y., Du, S., & Du, K. (2020). Evaluation and calibration of a low-cost particle sensor in ambient conditions using machine learning technologies. *Atmospheric Measurement Techniques*, *13*(4), 1693–1707. https://doi.org/10.5194/amt-2019-393

Snyder, E. G., Watkins, T. H., Solomon, P. A., Thoma, E. D., Williams, R. W., Hagler, G. S. W., et al. (2013). The changing paradigm of air pollution monitoring. *Environmental Science & Technology*, *47*(20), 11369–11377. https://doi.org/10.1021/es4022602

Stieb, D. M., Burnett, R. T., Smith-Doiron, M., Brion, O., Shin, H. H., & Economou, V. (2008). A new multipollutant, no-threshold air quality health index based on short-term associations observed in daily time-series analyses. *Journal of the Air & Waste Management Association*, *58*(3), 435–450. https://doi.org/10.3155/1047-3289.58.3.435

Strathcona Residents Association. (2021). Air quality monitoring project community survey report. (Technical Report). Retrieved from https://strathcona-residents.org/wp-content/uploads/2021/06/Community-Survey-Report.pdf

Su, J. G., Morello-Frosch, R., Jesdale, B. M., Kyle, A. D., Shamasunder, B., & Jerrett, M. (2009). An index for assessing demographic inequalities in cumulative environmental hazards with application to Los Angeles, California. *Environmental Science & Technology*, *43*(20), 7626–7634. https://doi.org/10.1021/es901041p

Tunno, B. J., Shields, K. N., Lioy, P., Chu, N., Kadane, J. B., Parmanto, B., et al. (2012). Understanding intra-neighborhood patterns in $PM_{2.5}$ and PM_{10} using mobile monitoring in Braddock, PA. *Environmental Health*, *11*(1), 76. https://doi.org/10.1186/1476-069X-11-76

Vancouver Fraser Port Authority. (2023). Strathcona area air quality study. Retrieved from https://portvancouver.civilspace.io/en/projects/strathcona-area-air-quality-study

Villa, F., & McLeod, H. (2002). Environmental vulnerability indicators for environmental planning and decision-making: Guidelines and applications. *Environmental Management*, *29*(3), 335–348. https://doi.org/10.1007/s00267-001-0030-2

Wang, M., Beelen, R., Basagana, X., Becker, T., Cesaroni, G., de Hoogh, K., et al. (2013). Evaluation of land use regression models for NO_2 and particulate matter in 20 European study areas: The ESCAPE project. *Environmental Science & Technology*, *47*(9), 4357–4364. https://doi.org/10.1021/es305129t

Wang, R., Henderson, S. B., Sbihi, H., Allen, R. W., & Brauer, M. (2013). Temporal stability of land use regression models for traffic-related air pollution. *Atmospheric Environment*, *64*, 312–319. https://doi.org/10.1016/j.atmosenv.2012.09.056

Wiebe, S. M. (2016). *Everyday exposure: Indigenous mobilization and environmental justice in Canada's chemical valley*. UBC Press.

Williams, R., Kilaru, V., Snyder, E., Kaufman, A., Dye, T., Rutter, A., et al. (2014). Air sensor guidebook. (Technical Report No. EPA/600/R-14/159).

Wu, Y., Hao, J., Fu, L., Wang, Z., & Tang, U. (2002). Vertical and horizontal profiles of airborne particulate matter near major roads in Macao, China. *Atmospheric Environment*, *36*(31), 4907–4918. https://doi.org/10.1016/S1352-2310(02)00467-3

Xia, Y., & Tong, H. (2006). Cumulative effects of air pollution on public health. *Statistics in Medicine*, *25*(20), 3548–3559. https://doi.org/10.1002/sim.2446

Xu, Y., Jiang, S., Li, R., Zhang, J., Zhao, J., Abbar, S., & González, M. C. (2019). Unraveling environmental justice in ambient $PM_{2.5}$ exposure in Beijing: A big data approach. *Computers, Environment and Urban Systems*, *75*, 12–21. https://doi.org/10.1016/j.compenvurbsys.2018.12.006

Zhou, P., Ang, B., & Poh, K. (2006). Comparing aggregating methods for constructing the composite environmental index: An objective measure. *Ecological Economics*, *59*(3), 305–311. https://doi.org/10.1016/j.ecolecon.2005.10.018

Zimmerman, N., Presto, A. A., Kumar, S. P. N., Gu, J., Hauryliuk, A., Robinson, E. S., & Subramanian, R. (2018). A machine learning calibration model using random forests to improve sensor performance for lower-cost air quality monitoring. *Atmospheric Measurement Techniques*, *11*(1), 291–313. https://doi.org/10.5194/amt-11-291-2018